

General One-Step Self-Assembly of Isostructural Intermetallic $\text{Co}^{\text{II}}\text{Ln}^{\text{III}}$ Cubane Aggregates

Pei Wang,[†] Santiranjan Shannigrahi,[‡] Nikolai L. Yakovlev,[‡] and T. S. Andy Hor^{*,†,‡}

[†]Department of Chemistry, National University of Singapore, 3 Science Drive 3, Singapore 117543, Singapore

[‡]Institute of Materials Research and Engineering, Agency for Science, Technology and Research, 3 Research Link, Singapore 117602, Singapore

S Supporting Information

ABSTRACT: A new family of Co/rare-earth intermetallic cubane aggregates $[\text{Co}_3\text{Ln}(\text{hmp})_4(\text{OAc})_5\text{H}_2\text{O}]$ (Ln = Dy, Ho, Er, Tm, Yb, Y) have been synthesized by self-assembly. Single-crystal X-ray diffraction analysis revealed that they are remarkably isostructural in showing a common $[\text{Co}_3\text{Ln}]$ core. Magnetic studies showed that the Dy, Er, Tm, Yb, and Y complexes are ferromagnetic. The Dy complex exhibits the largest magnetocaloric effect ($-\Delta S_m = 12.58 \text{ J kg}^{-1} \text{ K}^{-1}$), which can be attributed to the large magnetic density of Dy^{III} .

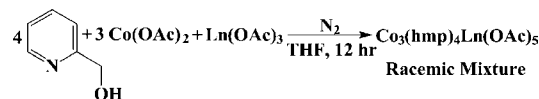
Intermetallic cubane is a special class of molecular materials that have niche applications in cluster catalysis,¹ up-conversion photoluminescence,² and molecular magnetism.³ Among the representative examples are $[\text{Cu}_3\text{Ln}]^4$ (Ln = Y, Gd), $[\text{Cu}_2\text{Dy}_2]$,⁵ $[\text{Mn}_2\text{Dy}_2]$,⁶ $[\text{Gd}_3\text{Fe}]$,⁷ $[\text{Co}_2\text{Ln}_2]$,⁸ (Ln = Gd, Dy, Ho, Tb, Y), and $[\text{Ni}_2\text{Ln}_2]$ ⁹ (Ln = Gd, Dy, Tb). The functions and applications of these materials hinge on the electronic character that the rare-earth element can bring to the cubane aggregate core and how such intermetallic hybridization can be controlled and harnessed. This challenge brings along a major obstacle to this field: how to keep the isostructural cubane framework and develop a controllable metal-substitution mechanism to replace a d-metal with an f metal. Realization of this form of molecular engineering would be considered as a major breakthrough because it could pave the way to “pick-and-choose” a heterometal to slot into a predetermined structural core and use the intermetallic and its cooperative effect with its d-metal neighbors to tune the functional outcomes. Unfortunately, this remains an elusive target because no such general method has been developed or reported. First, unlike ligand replacement, metal replacement is inherently difficult because the usual nucleophilic or electrophilic substitution is rarely suitable. There is, hence, no simple synthetic pathway to substitute d with f metal (e.g., from Co_4 to Co_3Ln) without disrupting the cubane framework. Second, self-assembly, simple as it is, does not usually drive toward a singular framework with specific intermetallic compositions because different metals tend to have different thermodynamic drivers.

In this Communication, we report a simple and effective self-assembly method for intermetallic cubanes that can be applied to a range of rare-earth metals. In this system, supported by the ligand 2-(hydroxymethyl)pyridine (hmpH), all metals examined converge to a desirable singular $[\text{Co}_3\text{Ln}]$ (Ln = Dy, Ho, Er, Tm,

Yb, Y) cubane core under standard self-assembly conditions. Using a single set of conditions, we are, hence, able to synthesize an array of isostructural intermetallic aggregates between Co^{II} and Ln^{III} and herein report their common crystallographic and structural features.

The mixtures of $\text{Co}(\text{OAc})_2$, $\text{Ln}(\text{OAc})_3$ (Ln = Dy, Ho, Er, Tm, Yb, Y), and hmpH^{10} in tetrahydrofuran are self-assembled in a stoichiometric ratio at room temperature in an inert atmosphere to afford pink-red solids of $[\text{Co}_3\text{Ln}]$ cubane aggregates (Scheme 1). All of them show a common parent peak of $[\text{Co}_3\text{Ln}-$

Scheme 1. Synthetic Scheme for 1–6 with Ln = Dy (1), Ho (2), Er (3), Tm (4), Yb (5), and Y (6)



$(\text{hmp})_4(\text{OAc})_4]^+$ in their electrospray ionization mass spectrometry (ESI-MS) spectra in CH_2Cl_2 (Figure S1 in the Supporting Information, SI). Attempts to introduce light lanthanide metals (Nd, Sm, Eu, Gd, or Tb) have failed to yield any desirable products, perhaps because of the strong structural distortion imposed by the large radius of these metals.

Single-crystal X-ray diffraction analysis of all of these new compounds, 1–6, has revealed that they are isostructural with a $[\text{Co}_3\text{Ln}]$ core, capped by four pyridylmethoxy O atoms to form a common heterocubane $[\text{Co}_3\text{LnO}_4]$ framework (the structure of 1 as a representative example is shown in Figure 1; other figures as well as bond and angle data are given in the SI). The $[\text{Co}_3\text{Ln}]$ core is supported by four pyridylmethoxide and five acetate ligands to maintain electroneutrality. Two of the octahedral Co^{II} atoms carry terminal pyridyl N atoms, thus leaving the third Co^{II} atom supported by a lone water molecule. The acetates are distributed as two chelating ligands on Ln^{III} , one bridging between the homometallic Co–Co pair, another across the intermetallic Co–Ln pair, and the last one serving as a unique unidentate ligand to fill the remaining vacant site on the hydrated Co^{II} center.

The Co–O [1.935(7)–2.251(8) Å] and Co–N [2.092(6)–2.159(5) Å] bonds are normal among octahedral Co^{II} complexes. The Ln–O bonds [2.274(4)–2.440(5) Å] decrease from 1 to 5, and those of 6 are similar to those of 2, which are attributed to

Received: July 13, 2012

Published: October 29, 2012

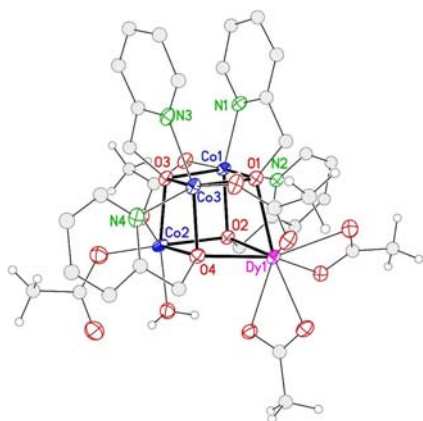
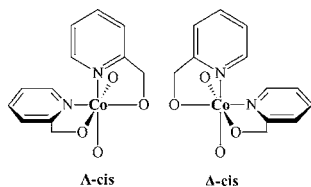


Figure 1. Molecular structure of the $\Lambda\Lambda$ isomer of **1** (hmp H atoms omitted for clarity). Color code: Dy, pink; Co, blue, O, red; N, green; C, gray; H, open circles.

lanthanide contraction. The $\text{Co}\cdots\text{Co}$ [3.0006(6)–3.2370(2) Å] and $\text{Co}\cdots\text{Ln}$ distances [3.318(1)–3.633(2) Å] are outside their formal bonding distances, suggesting that these cubanes are best treated as aggregates instead of clusters. The $\text{Co}\cdots\text{Co}$ distances are, however, shorter than the antiferromagnetic $\text{Co}\cdots\text{Co}$ distance of [Co_2Y_2] cubane⁸ [3.2409(8)–3.27(4) Å].

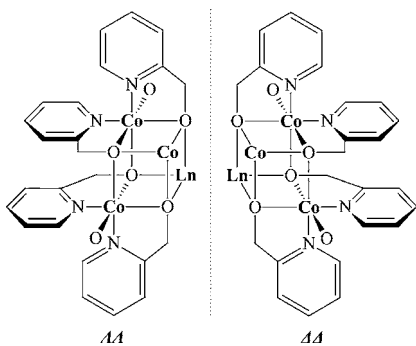
These molecules are inherently chiral, with nonsuperimposable mirror images (Figure S2 in the SI), but they are obtained as racemic mixtures. Each [$\text{Co}(\text{hmp})_2\text{O}_2$] unit is structurally distinguished as two enantiomers (Λ -cis and Δ -cis in Scheme 2). When they are assembled with the distinctive Co^{II} and Ln^{III} , it

Scheme 2. Structural Representations of the Enantiomeric Pairs of the Basic [$\text{Co}(\text{hmp})_2\text{O}_2$] Moiety (Ethyl Acetate Groups Are Omitted)



results in a racemic mixture of two homochiral ($\Lambda\Lambda$ and $\Delta\Delta$) frameworks (Scheme 3). Single-crystal analysis revealed that molecular equivalents of $\Lambda\Lambda$ -[Co_3Ln] and $\Delta\Delta$ -[Co_3Ln] are cocrystallized in an achiral crystal of the space group $P\bar{1}$ to form a

Scheme 3. Structural Representations of the Enantiomeric Pairs (Ethyl Acetate Groups Are Omitted) of the [Co_3Ln] Core



($\Lambda\Lambda/\Delta\Delta$)-[Co_3Ln] racemate. Attempts in racemic resolution by high-performance liquid chromatography are hampered by product decomposition in the chiral column.

Variable-temperature direct-current (dc) magnetic susceptibility data were collected for **1–6** from 300 to 4 K under an applied field of 0.1 T (Figure 2) using a vibrating sample

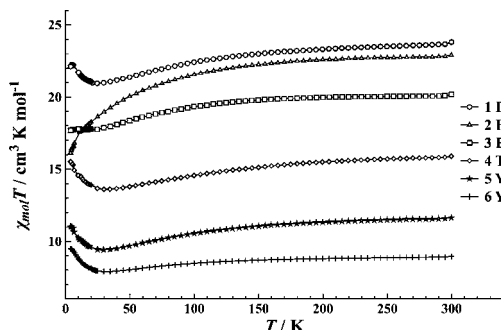


Figure 2. Plot of $\chi_{\text{mol}}T$ versus T under an applied dc field of 0.1 T for **1–6**.

magnetometer integrated with Quantum Design PPMS. The observed $\chi_{\text{mol}}T$ values at 300 K (Table 1) are larger than the spin-

Table 1. Magnetic Data of **1–6^a**

	1 (Dy)	2 (Ho)	3 (Er)	4 (Tm)	5 (Yb)	6 (Y)
$S(\text{Ln}^{3+})$	$5/2$	2	$3/2$	1	$1/2$	0
$S(\text{Co}^{2+})$	$3/2$	$3/2$	$3/2$	$3/2$	$3/2$	$3/2$
$L(\text{Ln}^{3+})$	5	6	6	5	3	
$J(\text{Ln}^{3+})$	$15/2$	8	$15/2$	6	$7/2$	
$g_f(\text{Ln}^{3+})$	$4/3$	$5/4$	$6/5$	$7/6$	$8/7$	
$g_f(\text{Co}^{2+})$	2	2	2	2	2	2
$\chi_{\text{mol}}T(\text{calcd})^b$	19.80	19.70	17.11	12.78	8.20	5.64
$\chi_{\text{mol}}T(\text{obs})^b$	23.82	22.93	20.18	15.90	11.66	8.95
$-\Delta S_{\text{m}}^c$	12.58	8.90	11.53	10.30	9.94	6.04

^a S , L , and J are quantum numbers for total spin angular momentum, total orbital angular momentum, and total angular momentum, respectively, of the ground multiplet. g_f is the Landé factor. ^bValues of $\chi_{\text{mol}}T$ are given in $\text{cm}^3 \text{K mol}^{-1}$. ^cMCE values $-\Delta S_{\text{m}}$ at 5.5 K for a field change of 7 T are given in $\text{J kg}^{-1} \text{K}^{-1}$.

only values calculated by Curie law using the relevant parameters S , L , J , and g_f . This is attributed to the significant orbital contributions of the high-spin Co^{II} centers with octahedral geometry.¹¹

The magnetic interaction between the Co^{II} centers in [Co_3Ln] can be studied with reference to the diamagnetic Y^{III} .^{8,12} As the sample of **6** is cooled, the $\chi_{\text{mol}}T$ value decreases gradually and reaches a round minimum of $7.90 \text{ cm}^3 \text{K mol}^{-1}$ at 30 K (Figure 2). Upon further cooling, the $\chi_{\text{mol}}T$ value increases rapidly, reaching a maximum value of $9.48 \text{ cm}^3 \text{K mol}^{-1}$ at 4 K. The decrease of $\chi_{\text{mol}}T$ from 300 to 30 K is due to the spin-orbit coupling of Co^{II} ,¹³ while the behavior from 30 to 4 K indicates overall ferromagnetic coupling between Co^{II} centers.¹⁴

The $\chi_{\text{mol}}T$ values of **1–5** decrease gradually from 300 to 30 K, which is due to the spin-orbit coupling of Co^{II} and Ln^{III} . Complexes **1**, **4**, and **5** show $\chi_{\text{mol}}T$ trends similar to that of **6**, in the 4–30 K range, which indicates the overall ferromagnetic couplings within the [Co_3Ln] cores. The $\chi_{\text{mol}}T$ values of **3** in the 4–30 K range reach a maximum of $17.77 \text{ cm}^3 \text{K mol}^{-1}$ at 10 K, indicating the very weak ferromagnetic couplings within the

[Co₃Er] cores. However, the $\chi_{\text{mol}}T$ values of **2** decrease abruptly from 30 K to its minimum at 4 K, which is due to either overall antiferromagnetic coupling within the [Co₃Ho] cores or depopulation of the low-lying excited states in the f shell of Ho^{III}.¹⁵ The decrease of $\chi_{\text{mol}}T$ values of **1** and **3** below their maxima may be traced to depopulation of the low-lying excited states in the f shell of Ln^{III}. Because both Co^{II} and Ln^{III} have complicated intrinsic magnetic characteristics including spin-orbit coupling and magnetic anisotropy, the intermetallic Co–Ln interactions are likely to be complex.⁸

Measurements of the field-dependent magnetizations (M) at low temperatures (4–8 K) were performed (complex **1** in Figure 3 and the others in Figure S3 in the SI). The magnetization values

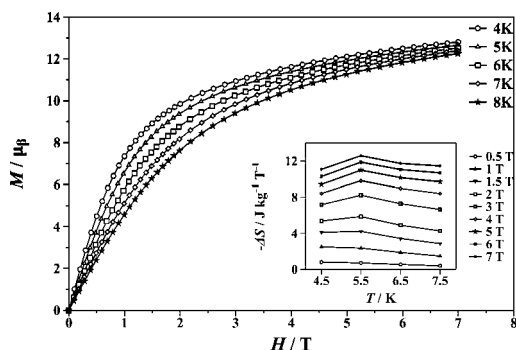


Figure 3. Field-dependent magnetization plots for **1** from 4 K to 8 K. Inset: Values of $-\Delta S_m$ calculated using the magnetization data for **1** at various fields (0.5–7 T) and temperatures (4.5–7.5 K).

at 4 K for all compounds are lacking in saturation of M versus H , and the magnetization values at 7 T are also lower than the expected saturation values. These phenomena indicate the presence of significant anisotropy and low-lying excited states of an ensemble of magnetic moments in each molecule.

Entropy changes were calculated for all of the compounds (Figure S3 in the SI) using the Maxwell equation as follows: $\Delta S_m(T)_{\Delta H} = \int [\partial M(T, H) / \partial T]_H dH$,¹⁶ and the magnetocaloric effect (MCE) values at 5.5 K for a field change $\Delta H = 7$ T are summarized in Table 1. The value of $-\Delta S_m$ for **1** reaches a maximum of 12.58 J kg⁻¹ K⁻¹ at 5.5 K. This is the largest magnitude among all of the [Co₃Ln] aggregates because Dy^{III} has a large magnetic density.¹² However, compared to the reported isotropic Gd^{III} compounds,^{11,12,17} the MCE values of **1** are much lower, which is attributed to the strong magnetic anisotropy of Dy^{III}.¹⁸ The frequency dependence of the out-of-phase (χ'') signal of **1** is characteristic of single-molecule magnetic behavior aroused from the magnetic anisotropy (Figure S4 in the SI).

In summary, we found that pyridyl-2-ylmethanoate (hmp) is a suitable ligand to promote the self-assembly of a series of isostructural heterometallic [Co₃Ln] (Ln = Dy, Ho, Er, Tm, Yb, Y) cubane aggregates. Unlike the known [Co₂Ln₂]⁸ series, the titled system converges to a common [Co₃Ln] core. The consistency across different rare-earth atoms is remarkable given that the synthetic method is exceptionally simple. These have provided a powerful means of tuning the magnetic properties of the aggregates (ferromagnet, weak ferromagnet, or antiferromagnet) by using different metal dopants.

■ ASSOCIATED CONTENT

Supporting Information

X-ray crystallographic data in CIF format, synthesis of all compounds, figures for ESI-MS, crystallographic data, figures for

crystal structures, and magnetization versus field curves. This material is available free of charge via the Internet at <http://pubs.acs.org>.

■ AUTHOR INFORMATION

Corresponding Author

*E-mail: andyhor@nus.edu.sg.

Notes

The authors declare no competing financial interest.

■ ACKNOWLEDGMENTS

This work was supported by National University of Singapore and A*STAR of Singapore (Grant R143-000-426-305). We thank Yimian Hong, Geok Kheng Tan, and Dr. Lip Lin Koh for determining the X-ray crystal structures. P.W. thanks the NUS Graduate School for Integrative Sciences and Engineering for a graduate scholarship.

■ REFERENCES

- (a) Mihara, H.; Xu, Y.; Shepherd, N. E.; Matsunaga, S.; Shibusaki, M. *J. Am. Chem. Soc.* **2009**, *131*, 8384–8385. (b) Handa, S.; Gnanadesikan, V.; Matsunaga, S.; Shibusaki, M. *J. Am. Chem. Soc.* **2010**, *132*, 4925–4934.
- (a) Torelli, S.; Imbert, D.; Cantuel, M.; Bernardinelli, G.; Delahaye, S.; Hauser, A.; Bunzli, J. C. G.; Piguet, C. *Chem.—Eur. J.* **2005**, *11*, 3228–3242. (b) Aboshyan-Sorgho, L.; Besnard, C.; Pattison, P.; Kittilstved, K. R.; Aebischer, A.; Bueznli, J. C. G.; Hauser, A.; Piguet, C. *Angew. Chem., Int. Ed.* **2011**, *50*, 4108–4112.
- (a) Gatteschi, D.; Sessoli, R. *Angew. Chem., Int. Ed.* **2003**, *42*, 268–297. (b) Evangelisti, M.; Brechin, E. K. *Dalton Trans.* **2010**, *39*, 4672–4676. (c) Sorace, L.; Benelli, C.; Gatteschi, D. *Chem. Soc. Rev.* **2011**, *40*, 3092–104.
- Aronica, C.; Chastanet, G.; Pilet, G.; Le Guennic, B.; Robert, V.; Wernsdorfer, W.; Luneau, D. *Inorg. Chem.* **2007**, *46*, 6108–6119.
- Aronica, C.; Pilet, G.; Chastanet, G.; Wernsdorfer, W.; Jacquot, J. F.; Luneau, D. *Angew. Chem., Int. Ed.* **2006**, *45*, 4659–4662.
- Mereacre, V.; Ako, A. M.; Clerac, R.; Wernsdorfer, W.; Hewitt, I. J.; Anson, C. E.; Powell, A. K. *Chem.—Eur. J.* **2008**, *14*, 3577–3584.
- Ako, A. M.; Mereacre, V.; Clérac, R.; Hewitt, I. J.; Lan, Y.; Anson, C. E.; Powell, A. K. *Dalton Trans.* **2007**, 5245–5247.
- Zhao, X. Q.; Lan, Y.; Zhao, B.; Cheng, P.; Anson, C. E.; Powell, A. K. *Dalton Trans.* **2010**, *39*, 4911–4917.
- Gao, Y.; Zhao, L.; Xu, X.; Guo, G. F.; Guo, Y. N.; Tang, J.; Liu, Z. *Inorg. Chem.* **2011**, *50*, 1304–1308.
- Experimentally, a slight excess (10%) of ligand is used to improve the product yield and minimize the byproducts of other cubanes.
- Zheng, Y.; Evangelisti, M.; Winpenny, R. E. P. *Chem. Sci.* **2011**, *2*, 99–102.
- Zheng, Y. Z.; Evangelisti, M.; Tuna, F.; Winpenny, R. E. *J. Am. Chem. Soc.* **2012**, *134*, 1057–1065.
- Bi, Y.; Wang, X.; Liao, W.; Wang, X.; Wang, X.; Zhang, H.; Gao, S. *J. Am. Chem. Soc.* **2009**, *131*, 11650–11651.
- (a) Ibrahim, M.; Lan, Y. H.; Bassil, B. S.; Xiang, Y. X.; Suchopar, A.; Powell, A. K.; Kortz, U. *Angew. Chem., Int. Ed.* **2011**, *50*, 4708–4711. (b) Galloway, K. W.; Schmidtman, M.; Sanchez-Benitez, J.; Kamenev, K. V.; Wernsdorfer, W.; Murrie, M. *Dalton Trans.* **2010**, *39*, 4727–4729.
- Zou, L.; Zhao, L.; Guo, Y.; Yu, G.; Guo, Y.; Tang, J.; Li, Y. *Chem. Commun.* **2011**, *47*, 8659–8661.
- (a) Karotsis, G.; Evangelisti, M.; Dalgarno, S. J.; Brechin, E. K. *Angew. Chem., Int. Ed.* **2009**, *48*, 9928–9931. (b) Sessoli, R. *Angew. Chem., Int. Ed.* **2012**, *51*, 43–45.
- Peng, J. B.; Zhang, Q. C.; Kong, X. J.; Zheng, Y. Z.; Ren, Y. P.; Long, L. S.; Huang, R. B.; Zheng, L. S.; Zheng, Z. *J. Am. Chem. Soc.* **2012**, *134*, 3314–3317.
- Karotsis, G.; Kennedy, S.; Teat, S. J.; Beavers, C. M.; Fowler, D. A.; Morales, J. J.; Evangelisti, M.; Dalgarno, S. J.; Brechin, E. K. *J. Am. Chem. Soc.* **2010**, *132*, 12983–12990.